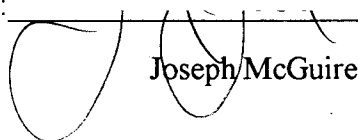


AN ABSTRACT OF THE THESIS OF

Jun Wang for the degree of Master of Science in Bioresource Engineering presented on August 31, 1995. Title: Surface Tension Kinetics of the Wild Type and Four Synthetic, Structural Stability Mutants of Bacteriophage T4 Lysozyme at the Air-water Interface.

Redacted for Privacy

Abstract approved:


Joseph McGuire

Surface tension kinetics exhibited by selected stability mutants of T4 lysozyme at the air-water interface were monitored with DuNoüy tensiometry. Mutant lysozymes were produced by substitution of isoleucine at position 3 with cysteine, leucine, tryptophan and glycine. Each substitution resulted in an altered structural stability quantified by a change in the free energy of unfolding. At a bulk concentration of 1.0 mg/ml, an analysis of surface tension kinetics using first-order rate equations yielded two rate constants, reflecting protein surface hydrophobicity and molecular weight, respectively. These rate constants varied little among the five T4 lysozyme variants. At a bulk concentration of 0.01 mg/ml, the same analysis gave one rate constant that correlated with protein structural stability. Additionally, the surface pressure kinetics were compared to the kinetic model evolving from a simple model for protein adsorption. This model allowed for parallel, irreversible adsorption into two states directly from solution, where state 2 molecules were more tightly bound to the surface and occupied greater interfacial area than state 1 molecules. The model indicated that less stable variants of T4 lysozyme have a greater tendency to adsorb in state 2, and state 2 molecules increase spreading pressure more than state 1 molecules occupying the same interfacial area. This phenomenon is more pronounced at lower concentration than at higher concentration.

Surface Tension Kinetics of the Wild Type and Four Synthetic,
Structural Stability Mutants of
Bacteriophage T4 Lysozyme at the Air-water Interface

by

Jun Wang

A THESIS

submitted to

Oregon State University

in partial fulfillment of
the requirements for the
degree of

Master of Science

Completed August 31, 1995
Commencement June, 1996

Master of Science thesis of Jun Wang presented on August 31, 1995

APPROVED:

Redacted for Privacy

Major Professor, representing Bioresource Engineering

Redacted for Privacy

Head of Department of Bioresource Engineering

Redacted for Privacy

Dean of Graduate School

I understand that my thesis will become part of the permanent collection of Oregon State University libraries. My signature below authorizes release of my thesis to any reader upon request.

Redacted for Privacy

Jun Wang, Author

ACKNOWLEDGMENT

I would like to thank Dr. Joseph McGuire, my major professor, for allowing me to perform this research at his lab as an exchange student, for his valuable guidance and support. I am grateful to Dr. Andrew G. Hashimoto, Dr. Henry W. Schaup, and Dr. William A. Atkinson for kindly serving as my committee members.

My appreciation is also extended to Dr. Cindy Bower and my fellow graduate students for their suggestions, friendship and support. Special thanks to Professor Matthews and Sheila Snow of the Institute of Molecular Biology, University of Oregon, for providing bacterial strains needed for this research, as well as Dr. David E. Williams, for allowing me to use facilities in his laboratory.

Without the financial support from the National Science Foundation and the Whitaker Foundation, this research would not have been completed.

Finally, I am indebted to Akademisches Auslandsamt of Stuttgart University and International Study Center of Oregon State University, for providing me the one-year exchange program. I also thank Wilhelm-Weckherlin-Stiftung in Stuttgart for personal financial support.

TABLE OF CONTENTS

	<u>Page</u>
1. INTRODUCTION	1
2. LITERATURE REVIEW	3
3. MATERIALS AND METHODS	9
3.1 The Stability Mutants of Bacteriophage T4 Lysozyme.....	9
3.2 T4 Lysozyme Production and Purification.....	12
3.3 DuNoüy Ring Tensiometry.....	15
3.4 Measurement of Surface Tension Kinetics.....	16
4. RESULTS AND DISCUSSION	19
4.1 Surface Tension Kinetics.....	19
4.2 Analysis with Reference to a Simple Kinetic Model.....	27
4.2.1 Parameter estimation.....	28
4.2.2 Model equations and the rate constants.....	32
4.3 Mass Transfer Limitations and the Low Concentration Data.....	36
5. CONCLUSION	45
BIBLIOGRAPHY	46

LIST OF FIGURES

<u>Figure</u>	<u>Page</u>
3.1	The α -carbon backbone of the wild type bacteriophage T4 lysozyme..... 10
3.2	A cross sectional view of the submerged ring..... 16
4.1	Surface tension kinetics of T4 lysozyme and the four stability mutants at a concentration of 0.01 mg/ml..... 20
4.2	Surface tension kinetics of T4 lysozyme and the four stability mutants at a concentration of 1.0 mg/ml..... 21
4.3	Analysis of kinetic plots for each protein at 1.0 mg/ml according to Eq. [4.1]..... 25
4.4	A simple mechanism for T4 lysozyme adsorption into one of two states defined by fractional surface coverages θ_1 and θ_2 27
4.5	Surface pressure kinetics at a bulk concentration of 1.0 mg/ml, The lines follow Eq. [4.10]..... 35
4.6	Surface pressure kinetics at a bulk concentration of 0.01 mg/ml, along with the surface pressure predicted with Eq. [4.14]..... 38
4.7	Analysis of kinetic plots for each protein at 0.01 mg/ml according to Eq. [4.1]..... 40
4.8	Surface pressure kinetics at a bulk concentration of 0.01 mg/ml. The lines follow Eq. [4.10]..... 44

LIST OF TABLES

<u>Table</u>		<u>Page</u>
3.1	Thermal stability of lysozymes with different amino acids at position 3.....	11
3.2	Range of stock protein concentrations used in the experiments.....	15
4.1	First-order rate constants K_1 and K_2 for each protein at 1.0 mg/ml.....	26
4.2	Estimation of θ_1 , θ_2 and Π at steady state for wild type, Ile3 \rightarrow Trp and Ile3 \rightarrow Trp (S-S).....	30
4.3	Estimated values of Π_{\max} and b at bulk concentration of 1.0 mg/ml.....	31
4.4	Value of the adsorption rate constants defined in Fig. 4.4, along with the value of $\Delta\Delta G$ for each protein.....	34
4.5	Value of the first-order rate constants K , along with the value of $\Delta\Delta G$ for each protein.....	39
4.6	Estimated values of Π_{\max} and b at 0.01 mg/ml.....	41
4.7	Value of the adsorption rate constants at 0.01 mg/ml, defined in Fig. 4.4, along with the value of $\Delta\Delta G$ for each protein.....	43

SURFACE TENSION KINETICS OF THE WILD TYPE AND FOUR SYNTHETIC, STRUCTURAL STABILITY MUTANTS OF BACTERIOPHAGE T4 LYSOZYME AT THE AIR-WATER INTERFACE

CHAPTER 1 INTRODUCTION

The behavior of proteins at interfaces is of relevance in natural and technical processes (1). Protein adsorption at the air-water interface is important in various biological, medical and technological systems, and has been widely studied for several decades (2-14). Mixtures of different proteins are usually involved in practical systems, and the adsorption of protein molecules alters interfacial properties significantly. For example, stabilization of foams using proteins is practiced in the food industry, and protein functionality in this context is strongly related to its adsorption at the air-water interface. Kitabatake *et al.* (2,3) examined the relationship between foamability, determined by a dimensionless term "foaming power", and surface tension of food protein solutions. They found that the first-order rate constant of surface tension decay, a result of protein adsorption, was closely correlated with solution foamability.

The study of molecular influences on protein adsorption is of prime interest due to its potential for providing a better understanding of adsorption competition in complex mixtures. Since proteins are themselves complex macromolecules, many molecular properties such as size, charge, shape, hydrophobicity and flexibility, can affect their adsorption behavior (18-20). Some researchers are currently using well-characterized proteins (6), or genetic variants from site-directed mutagenesis (9, 21) as model proteins to study the behavior of proteins at interfaces. Although it may seem far removed from circumstances encountered in practice, examination of relatively simple, well defined

systems holds much promise for gaining a better quantitative understanding of adsorption mechanism.

Water molecules at the air-water interface are in a state of higher free energy than their counterparts in the bulk because they have fewer nearest neighbor interactions than bulk molecules. This amount of excess surface free energy is considered to be the air-water surface tension. The adsorption of proteins at the air-water interface, and their subsequent conformational changes act to minimize interfacial free energy. Since surface tension kinetics are closely related to protein adsorption at the air-water interface, the changes in surface tension provide a convenient way of monitoring penetration into the surface and conformational rearrangements of adsorbed protein molecules.

The goal of this research was to gain a better understanding of structural stability influences on adsorption by studying the adsorption of stability mutants of a single protein that differ insignificantly with respect to other properties such as charge, surface hydrophobicity, three-dimensional structure and molecular weight. In this research, the wild type and four single-site mutants of bacteriophage T4 lysozyme were selected to study the effects of structural stability on adsorption to the air-water interface by measuring surface tension kinetics. In the following chapter a summary of related studies as well as some kinetic models for adsorption are presented.

CHAPTER 2

LITERATURE REVIEW

Researchers today are taking advantage of the availability of well-characterized proteins, as well as genetic variants and site-directed mutants of single proteins, to make significant advances in the study of protein adsorption at interfaces.

Hunter *et al.* (4, 5) determined the adsorption isotherms of chicken egg white lysozyme and β -casein at the air-water interface by using a radiotracer technique. They observed monolayer saturation at a low bulk concentration and multilayer adsorption at a high concentration of protein in the bulk. Through sequential protein adsorption experiments they found that β -casein adsorbed at the interface in any layer was exchangeable with that in the bulk solution. While lysozyme molecules adsorbed in the layer adjacent to the interface exchanged insignificantly with those in the bulk solution. An abrupt increase in surface concentration with increasing bulk concentration were observed in the isotherm data indicating that protein could adsorb in different orientations in one layer: side-on or end-on.

Wei *et al.* (6) measured the surface tension kinetics for five model proteins (superoxide dismutase, cytochrome-c, myoglobin, lysozyme and ribonuclease-A) at bulk concentrations of 0.01 mg/ml and 1.0 mg/ml using the Wilhelmy Plate method to determine the relationship between kinetics, stability, and hydrophobicity of each protein. At low protein concentration (0.01 mg/ml), an "induction period" was observed, where the surface tension did not change in the first few minutes of the experiments. Following the induction period, the change in surface tension followed first-order kinetics. They found that the induction period at 0.01 mg/ml bulk concentration was related to protein conformational stability, with more stable proteins having longer induction periods. Additionally, when the surface tension kinetics were compared, they found that

stable proteins had lower first-order rate constants than less stable proteins. No induction periods were observed at high bulk concentration (1.0 mg/ml). The surface tension kinetics consisted of an initial rapid decrease followed by a much slower decrease. The two rate constants describing these two different kinetic components were considered to reflect the surface hydrophobicity and the chain length of the protein.

The changes in surface pressure of several single point mutants of human hemoglobin were determined by Elbaum *et al.* (7). Their results showed that mutants containing the glutamic acid \rightarrow valine substitution at the $\beta 6$ position, characteristic of both hemoglobin S and hemoglobin C_{Harlem}, exhibited faster kinetics and a greater spreading pressure at apparent equilibrium than hemoglobin A and other variants. Electrostatic, hydrogen bonding and hydrophobic interactions are among the main factors which affect the surface activity of a hemoglobin molecule. They concluded that the different interfacial behavior between the oxy forms of hemoglobin A and hemoglobin S could be the determining factor for their differences in mechanical precipitations, such as mixing, stirring, or shaking.

By using a radiotracer method Xu and Damodaran (8) studied the adsorption kinetics of ^{14}C -labeled native, partially and fully denatured hen, human, and bacteriophage T4 lysozymes at the air-water interface. They observed substantial differences in adsorption dynamics among the three variants, and proposed a general mechanism of protein adsorption at interfaces. The driving force for adsorption of proteins was considered to be not only the concentration gradient, but also the interfacial force field consisting of several molecular potentials, such as the hydrophobic, electrostatic, hydration, and conformational potentials.

Kato and Yutani (9) measured the surface tension, foaming, and emulsifying properties of wild-type and six mutants of tryptophan synthase α -subunits, produced by single amino acid substitution at position 49 in the interior. The Gibbs free energy of denaturation in water (ΔG_{water}) varied from about 5 to 17 kcal/mol, depending on the

residue substitution at position 49. They observed that these measured surface properties correlated well with the values of ΔG_{water} . In particular, they found that more stable mutants showed less surface activity, leading to the conclusion that protein surface properties are determined to some extent by their conformational stabilities.

Much work has been done in the area of modeling protein adsorption, focusing on both adsorption isotherms and adsorption kinetics.

Hunter *et al.* (4, 5) developed an isotherm model for the chicken egg white lysozyme and β -casein adsorption at air-water interface by dividing the adsorption isotherm into three regions: side-on adsorption, end-on adsorption and multilayer adsorption. For the side-on adsorption, for example, Langmuirian kinetics were used, with the adsorption rate being proportional to bulk concentration and available surface area, and the desorption rate proportional to the amount adsorbed at the interface:

$$\frac{d\Gamma_1'}{dt} = k_1' \exp(-E_a' / RT) C(1 - \hat{a}' \Gamma_1') - k_{-1}' \exp(-E_d' / RT) \Gamma_1'. \quad [2.1]$$

In Eq. [2.1], Γ_1' is the surface concentration of side-on adsorbed protein, C is the bulk concentration, and \hat{a}' is the average area occupied per molecule. k_1' , k_{-1}' , E_a' , and E_d' are the preexponential factors and energies of activation for adsorption and desorption, respectively. The model fit the isotherm data quite well in each region, and it was able to predict the abrupt increase in surface concentration.

Earlier, Guzman *et al.* (10) introduced a similar adsorption isotherm model, and fit it to data obtained by Graham and Philips (11, 12) for three different proteins, including lysozyme. They considered protein transport from bulk solution to the air-water interface as an infinite-medium molecular diffusion. The partial differential equation describing one-dimensional diffusion of proteins in a semi-infinite fluid was written as:

$$\frac{\partial c_p}{\partial t} = D_p \frac{\partial^2 c_p}{\partial x^2} \quad [2.2]$$

In the above equation, the origin of the x axis is the air-water interface, D_p is the diffusion coefficient of protein in solution and c_p is the bulk concentration. With the appropriate initial and boundary conditions they solved the equation by an explicit finite difference method. Since the experimental mass transfer rate was much faster than predicted by diffusion, they modeled the transport of protein by an effective mass transfer coefficient, which could have resulted from small temperature gradients in the bulk during the experiment in addition to the diffusion.

Narsimhan and Uraizee (13) studied globular protein adsorption at an air-water interface, and described the adsorption kinetics as a one-dimensional diffusion of protein molecules in a potential field as defined in the following equation:

$$\frac{\partial}{\partial t} c(x, t) = \frac{\partial}{\partial x} \left[D \frac{\partial}{\partial x} c(x, t) + \frac{D}{kT} c(x, t) \frac{d\phi(x)}{dx} \right], \quad [2.3]$$

where D is the diffusion coefficient, $c(x, t)$ is the protein concentration at time t at a distance x from the interface, k is the Boltzmann constant, T is the temperature, and $\phi(x)$ is the interaction potential experienced by the protein molecule. Factors which were considered to contribute to the potential field included electrostatic interactions, energy required to clear sufficient interfacial area for anchoring the molecules, and the change in free energy due to exposure of surface hydrophobic functional groups to air. It was concluded that proteins with larger surface hydrophobicities and smaller size would exhibit faster adsorption kinetics.

Based on the model developed by Guzman *et al.* (10), a more complex model was suggested by Douillard *et al.* (14), allowing for a double layer adsorption of protein. The

first layer of protein in two different conformations could reach a saturation, however the second layer, with less specifically adsorbed protein, could not reach saturation. For evaluation the models were fit to surface concentration isotherms and surface pressure isotherms of several proteins obtained by Graham and Philips (12). The model parameters determined from concentration or pressure isotherms were in good agreement, indicating that both types of isotherm are relevant to the same model.

Lundström (15) was the first researcher who introduced multi-state modeling of protein adsorption at interfaces. Krisdhasima *et al.* (16, 17) adapted that development to describe the adsorption kinetics of β -lactoglobulin at silanized silica surfaces, and the surfactant-mediated removal of selected milk proteins from silanized silica surfaces. They proposed a two step mechanism for irreversible protein adsorption. In step 1, the protein molecule adsorbs reversibly to the surface after a short contact time, and adopts a surface conformation close to its native form. In step 2, the reversibly adsorbed molecule undergoes a surface-induced conformational change and reaches an irreversibly adsorbed form. Protein molecules were allowed to desorb into the bulk solution in the first step. Neglecting the influence of diffusion, equations describing the time-dependent fractional surface coverage of protein in each of the two states, one reversibly adsorbed (θ_1) and one irreversibly adsorbed (θ_2), were written as

$$\frac{d\theta_1}{dt} = k_1 C (1 - \theta_1 - \theta_2) - (k_{-1} + s_1) \theta_1 \quad [2.4]$$

and

$$\frac{d\theta_2}{dt} = s_1 \theta_1, \quad [2.5]$$

where C is the bulk protein concentration, k_1 , k_{-1} and s_1 are the rate constants for adsorption, desorption and conversion from state 1 to state 2, respectively.

The ranking of the rate constants defining protein adsorption and conversion to a more-tightly bound stage was possible by using the single-component adsorption data and the elutability of each adsorbed protein from a silica surface using sodium dodecylsulfate. It was consistent with protein molecular properties such as surface hydrophobicity, size and prolate orientation which affect the surface activity of each protein. They found that at high protein bulk concentration (1.0 mg/ml) the diffusion controlled transport of protein from the bulk to the surface did not limit the adsorption. In that work it was shown that the use of a simple mechanism to interpret experiments provides a powerful tool in understanding the course of protein adsorption.

McGuire *et al.* (21) observed different surface behaviors among bacteriophage T4 lysozyme and three of its stability mutants during single-component adsorption and dodecyltrimethylammonium-bromide-mediated elution experiments. The resistance to elutability was observed to be correlated to protein stability. A kinetic model was proposed which allowed proteins to adsorb directly onto the surface in two differently bound states from the bulk solution. The ratio of the adsorbed mass of these two protein states in the monolayer were estimated for the wild type and two mutants using the experimental data. The calculated fraction of more tightly bound molecules clearly increased with decreasing protein structural stability. In general, thermal stability is an important property at interfaces, and variants of bacteriophage T4 lysozyme are excellent model proteins for the study of stability influences on protein interfacial behavior.

CHAPTER 3

MATERIALS AND METHODS

3.1 The Stability Mutants of Bacteriophage T4 Lysozyme

Phage lysozyme is a hydrolytic enzyme that cleaves glycosidic bonds in the bacterial cell wall, and leads to cell lysis (22). Bacteriophage T4 lysozyme was chosen in this research as the model protein because it is extremely well characterized: the protein's 3-D structure and surface morphology are known, and numerous variants of this protein have been produced through site-directed mutagenesis and characterized with respect to their deviations in crystal structure and thermodynamic stability from the wild type.

T4 lysozyme has 164 amino acids, a molecular weight of approximately 18,700 Daltons and a size of about 50x30x30Å (23). It is a basic molecule with isoelectric point above 9.0 and an excess of nine positive charges at neutral pH. The use of T4 lysozyme variants with single amino acid substitutions is very useful for studying the molecular basis of protein behavior, since they can be synthesized to differ significantly from each other in only one aspect, such as conformational stability.

A schematic of the α -carbon backbone of T4 lysozyme, illustrated in Fig. 3.1, shows that the molecule has two distinct domains, the C-terminal and N-terminal lobes, which are joined by an α -helix (residues 60-80) that traverses the length of the molecule (24).

Isoleucine at position 3 has been replaced with 13 different amino acid residues by site-directed mutagenesis (25). In that work it was shown that hydrophobicity of the residue at position 3 influences the stability of the whole molecule, since Ile 3 contributes to the major hydrophobic core of the C-terminal lobe and also helps to link the N- and C-terminal domains. The side chain of Ile 3 contacts the side chains of methionine at

position 6, leucine at position 7, and isoleucine at position 100; it also contacts the main chain of cysteine at position 97. The differences in structural stability among the mutants are given by $\Delta\Delta G$: the difference between the free energy of unfolding of the mutant protein and that of the wild type at the melting temperature of the wild-type lysozyme.

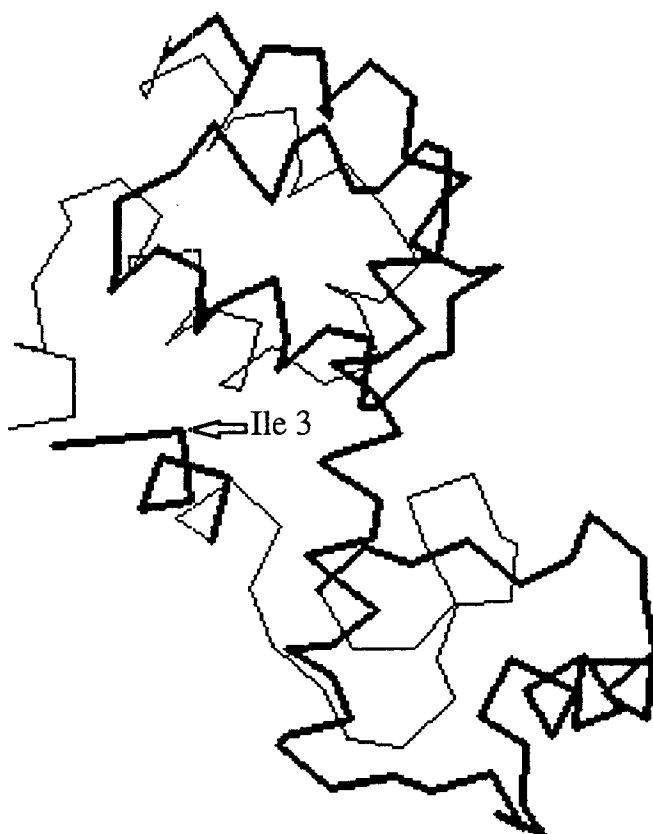


Figure 3.1. The α -carbon backbone of the wild type bacteriophage T4 lysozyme.

Four stability mutants plus the wild type lysozyme were selected for this project. The thermal stabilities of these lysozyme variants are shown in Table 3.1 (25). A positive value of $\Delta\Delta G$ indicates that the mutant is more stable than the wild type, and a negative $\Delta\Delta G$ corresponds to lower stability. The substitution with cysteine for Ile 3 (Ile3 \rightarrow Cys(S-S)) allows a disulfide linkage formation between Cys 3 and Cys 97, which leads to increased stability for this mutant. The enhanced stability of the Ile3 \rightarrow Leu mutant seems to be a result of an increase in hydrophobic stabilization (25). The replacement with Trp and Gly at position 3 causes unfavorable steric interactions, unsatisfied hydrogen bonds and differences in van der Waals interactions in addition to the hydrophobic effect due to their side chains, and therefore these variants are less stable. Substitution at position 3, so near the amino terminus, can be made without major changes in the protein structure (25).

Table 3.1. Thermal stability of lysozymes with different amino acids at position 3 (25).

Amino acid at position 3	$\Delta\Delta G$ (kcal/mol) at pH=6.5
Trp	-2.8
Gly	-2.1
Wild type	0.0
Leu	0.4
Cys (S-S)	1.2

3.2 T4 Lysozyme Production and Purification

The production of synthetic mutants of T4 lysozyme was performed using transformed cultures of *Escherichia coli* strain RR1. Individual bacteria strains, containing the mutant lysozyme expression vectors desired for this work, were stored at -80°C and originally provided by Professor Brian Matthews and co-workers at the Institute of Molecular Biology, University of Oregon, Eugene, OR.

Expression and purification of the mutant lysozymes were performed following established procedures (24).

Cells bearing the desired mutant lysozyme expression vector, which carried an ampicillin resistant gene and was controlled by the *lac i* repressor, were grown first overnight (about 8 h) in 100 ml of sterilized LBH broth (1 g tryptone, 0.5 g yeast extract, 0.5 g NaCl, 0.1 ml 1 N NaOH, and 100 ml deionized distilled water (DDW)) containing 10 mg of ampicillin at 37°C. This culture was then added to a 7-liter autoclaved fermenter filled with about 4.8 liters of sterilized LB broth (57.6 g tryptone, 24 g yeast extract, 48 g NaCl, 4.8 g glucose, and 4.8 L DDW) with 400 mg of ampicillin and 1.5 ml tributyl phosphate (Sigma Chemical Co., St. Louis, MO) and grown at 35°C by using a water bath with a circulating system (Model 1120, VWR Scientific, Portland, OR). Agitation was maintained at 600 rpm with a speed controller (ADI 1012, Applikon Dependable Instruments, Schiedam, Holland) while the air flow rate was maintained at 0.8 kg/s. When the optical density at 595 nm (DU 62 Spectrophotometer, Beckman Instruments, Inc., Fullerton, CA) was about 0.8 (requiring about 2 h), lysozyme expression was induced by the addition of 750 mg of isopropyl- β -thiogalactoside (IPTG, Sigma Chemical Co., St. Louis, MO) dissolved in 10 ml DDW, and then introduced into the growth media. The temperature was lowered to 30°C, and a further fermentation of about 110 minutes was allowed with an air flow rate of 0.52 kg/s, and an agitation of 200 rpm. The cells were then harvested and centrifuged at 4°C, 13k rpm (JA-14 Rotor, Beckman Model J2-MI

Centrifuge, Beckman Instruments, Inc., Palo Alto, CA) for 25 minutes. From this point, all purification procedures were performed at 4°C unless otherwise indicated.

Mutant proteins were purified from both the pellet and supernatant fractions. Supernatant was re-centrifuged at 13k rpm for 40 minutes, and the second-spin pellet was discarded. The first-spin pellets were combined and resuspended with 20 ml of 10 mM Tris buffer, pH 7.4. Lysis buffer (0.1 M sodium phosphate buffer, 0.2 M NaCl, 10 mM MgCl₂, pH 6.6) was added to a final volume of about 200 ml, followed by the addition of 1 ml of 0.5 M ethylenediamine tetraacetic acid (EDTA, Sigma Chemical Co.), pH 8.0, to each 100 ml of resuspended pellet. The suspension was stirred overnight (about 12 hours), after which about 0.01 mg of deoxyribonuclease I (Dnase I; crude powder from bovine pancreas, Sigma Chemical Co.) and 1 ml of 1 M MgCl₂ were added to each 100 ml of pellet solution. This was stirred at room temperature for 2 hours, followed by a centrifugation at 20k rpm (JA-20 Rotor, Beckman Model J2-MI Centrifuge, Beckman Instruments, Inc., Palo Alto, CA) for 30 minutes. The supernatant was combined with that from the original centrifugation, and the pellet this time was discarded.

Each 1100 ml of combined supernatant was dialyzed in 1200 ml fleakers against about 4 liters of deionized, distilled water, using Spectra/Por regenerated cellulose (RC) hollow fiber bundles (MWCO 18,000, Spectrum Medical Industries, Inc., Houston, Texas) until its conductivity was between 2 and 3 µmho/cm. Its pH was then adjusted to between 6.5 and 7.5 (with 1 N NaOH or 1 N HCl if needed). This process required about 48 hours.

The dialyzed supernatant was loaded onto a CM Sepharose ion exchange column (CM Sepharose CL-6B CCL-100, Sigma Chemical Co.), previously equilibrated with 50 mM Tris buffer, pH 7.25. After loading the column, a thick white band of protein at the top of column bed could be observed.

The Sepharose column was rinsed with 150 to 200 ml of 50 mM Tris buffer until the column was clear. A salt gradient from 0.05 to 0.30 M NaCl in 50 mM Tris was used to elute the lysozyme protein into a fraction collector (Frac-100, Pharmacia LKB Biotechnology, Alameda, CA). The eluant was monitored with a UV monitor (Optical unit UV-1 and Control unit UV-1, Pharmacia LKB Biotechnology), and output was recorded on a chart recorder. The fractions containing protein were combined in Spectra/Por molecular porous membrane tubing (MWCO 12-14K, Spectrum Medical Industries, Inc.), and dialyzed against 50 mM sodium phosphate buffer (20× eluant volume), pH 5.8, containing 0.02% sodium azide (NaN_3) for about 12 hours.

Protein solution was concentrated using a SP Sephadex column (SP Sephadex C50, Sigma Chemical Co.). Mutant proteins were eluted with 0.10 M sodium phosphate, pH 6.5, containing 0.55 M NaCl, and 0.02% NaN_3 . The exact concentration of the proteins was determined by measuring optical density at 280 nm with a Beckman UV spectrophotometer (Model DU-62, Beckman Instruments, Inc., Fullerton, CA) after being diluted 1:100 with 0.10 M sodium phosphate buffer, pH 6.5, then dividing OD by 1.28 for all variants except Ile3 → Trp (divided by 1.46). The yield of lysozyme was usually between 20 (Ile3 → Gly) and 150 mg (wild type). Preparations were stored in 1.5 ml vials without further treatment at 4°C and used within a week. SDS-gel electrophoresis showed the presence of only one band (30); the isolated proteins were on the average over 95% pure with a remaining fraction consisted of salts and peptide fragments. No evidence suggests that the make-up of this fraction was mutant-specific, or that it influenced any of the trends observed in the experiments. Table 3.2 shows the range of stock concentrations in the vials used in the experiments for each protein.

Table 3.2. Range of stock protein concentrations used in the experiments.

Amino acid at position 3	Range of concentrations (mg/ml)
Trp	3.3 - 35
Gly	2.3 - 12.3
Ile	5.7 - 82.5
Leu	3.4 - 45.2
Cys (S-S)	3.4 - 70.3

3.3 DuNoüy Ring Tensiometry

In this work a DuNoüy tensiometer (Model 70535, CSC Scientific Co., Inc., Fairfax, VA) was used to determine the surface tension. The tensiometer employs the "ring method" of measurement, which is widely accepted as a method giving satisfactory results for colloidal suspensions (26). It allows measurements to be made in a short time and with high precision (27).

To determine the surface tension, the ring is dipped into the liquid and then raised until the liquid collar, which comes up with the ring, collapses. The force required to lift the ring is measured, and is equal to the downward pull resulting from surface tension γ (after calibration 26, 27). Figure 3.2 shows a cross sectional view of a submerged ring with the liquid collar. The value of the surface tension given by the scale reading of the tensiometer is however an "apparent surface tension", since the hydrostatic weight of the liquid underneath the ring is included. To obtain the true surface tension, it is necessary to multiply the apparent surface tension by a correction factor which can be estimated by using the equation of Zuidema and Waters, presented in graphical form (26).

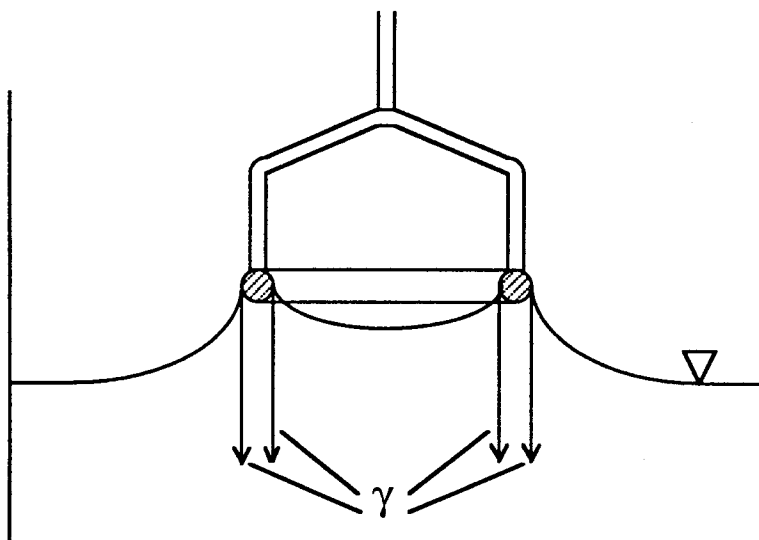


Figure 3.2. A cross sectional view of the submerged ring. The arrows indicate the force resulting from surface tension γ .

3.4 Measurement of Surface Tension Kinetics

All the experiments were carried out at a controlled room temperature (22 to 23°C). First the lysozyme solutions were diluted to the desired concentration with 0.01 M sodium phosphate buffer, pH 7.0. Buffer solution was prepared by titration of 0.01 M sodium phosphate monobasic monohydrate ($\text{NaH}_2\text{PO}_4 \cdot \text{H}_2\text{O}$) and 0.01 M sodium phosphate dibasic heptahydrate ($\text{Na}_2\text{HPO}_4 \cdot 7\text{H}_2\text{O}$) (Mallinckrodt Specialty Chemical Co., Paris, Kentucky). A solution of 0.02% (mass/volume) of sodium azide (NaN_3) (EM Science, Cherry Hill, N.J.) was then added as an anti-microbial agent.

In this research two protein concentrations (0.01 mg/ml and 1.0 mg/ml) were used. Each experiment required 70-120 ml of protein solution. For the low concentration proteins were generally taken from the stock vials with the highest concentrations, and stock vials with all different concentrations within the range shown in Table 3.2 were

used to make the high protein concentration solutions, since a large amount of protein was required (70 mg). Because the protein concentration differed among the stock vials, the remaining fraction consisting of salts and peptide fragments differed negligibly in the final protein solutions of low concentration (0.01 mg/ml), but quite significantly in the solutions of high concentration (1.0 mg/ml). The variation did not influence the results however, since replicate experiments produced consistent values (± 0.2 mN/m) despite any batch to batch differences which may have been present.

The buffer and protein mixture was gently stirred with a magnetic stirrer for about 2 minutes. An experiment began with the addition of 15-20 ml of protein solution into Rodac plate covers (Becton-Dickinson & Co., Oxnard, CA). A DuNoüy platinum-iridium ring was carefully cleaned between each measurement by rinsing it in ethanol and deionized, distilled water followed by flaming in the oxidizing portion of the flame of an alcohol burner until the ring was "red" hot. A cover containing the protein solution was then gently placed on the sample table of the tensiometer, and the ring was hung from the load cell and lowered about 5 mm below the surface of the liquid. The ring was pulled from the surface and the apparent surface tension recorded. Care was taken to ensure consistency in pulling the ring from the liquid for each measurement.

Several covers containing the same protein solution were used sequentially in order to give each surface at least 30 minutes to recover from the disturbance caused by the measurement. In all cases, the first measurement could be completed within about 2 min after introducing the protein solution, and measurements were taken every 10 to 20 min from the beginning until the end of each experiment. Five replicates were performed for each experiment.

The major error associated with the experiments was the perturbation of the air-water interface after each measurement. The ring was pulled from the surface until the liquid collar collapsed, resulting in surface turbulence which slightly disrupted the adsorbed protein layer. Up to five measurements were taken from each cover per

experiment, although a recovery time of at least 30 minutes was allowed between measurements.

CHAPTER 4

RESULTS AND DISCUSSION

4.1 Surface Tension Kinetics

An average was taken from the five surface tension kinetic plots obtained for each protein at the air-water interface. The results are shown in Figs. 4.1 and 4.2. It is apparent that the surface tension of the protein solutions decreased with time and approached steady state after about 1.5 h at a bulk concentration of 1.0 mg/ml, and about 4 h at a concentration of 0.01 mg/ml.

The air-water interface is not just a simple geometrical plane between two homogeneous phases, but rather a film of a characteristic thickness. In a protein solution the protein molecules can diffuse to and penetrate the interface via driving forces arising from hydrophobic and electrostatic interactions (8), and temperature gradients (10). After they reach the air-water interface, their hydrophilic groups remain in the water, while the hydrophobic chains can escape into the air phase through conformational rearrangement, where they are energetically more welcome than in the water. Therefore the protein molecules tend to accumulate at the surface forming one or more molecular layers, and this process is called adsorption. The net result of the protein adsorption is that the surface tension is lowered (11). The more amino acid residues of protein molecules that are packed into the interface, the lower the surface tension, until the surface is saturated.

The results of these experiments were consistent with adsorption kinetic data obtained by Wei *et al.* (6) using egg-white lysozyme, and Xu and Damodaran (8) using egg-white, human and T4 phage lysozymes at the air-water interface, with the exception of an induction period reported in both studies at low concentration (0.01 mg/ml (6) and 0.0015 mg/ml (8)), but not seen in our data. Wei *et al.* (6) explained the existence of the

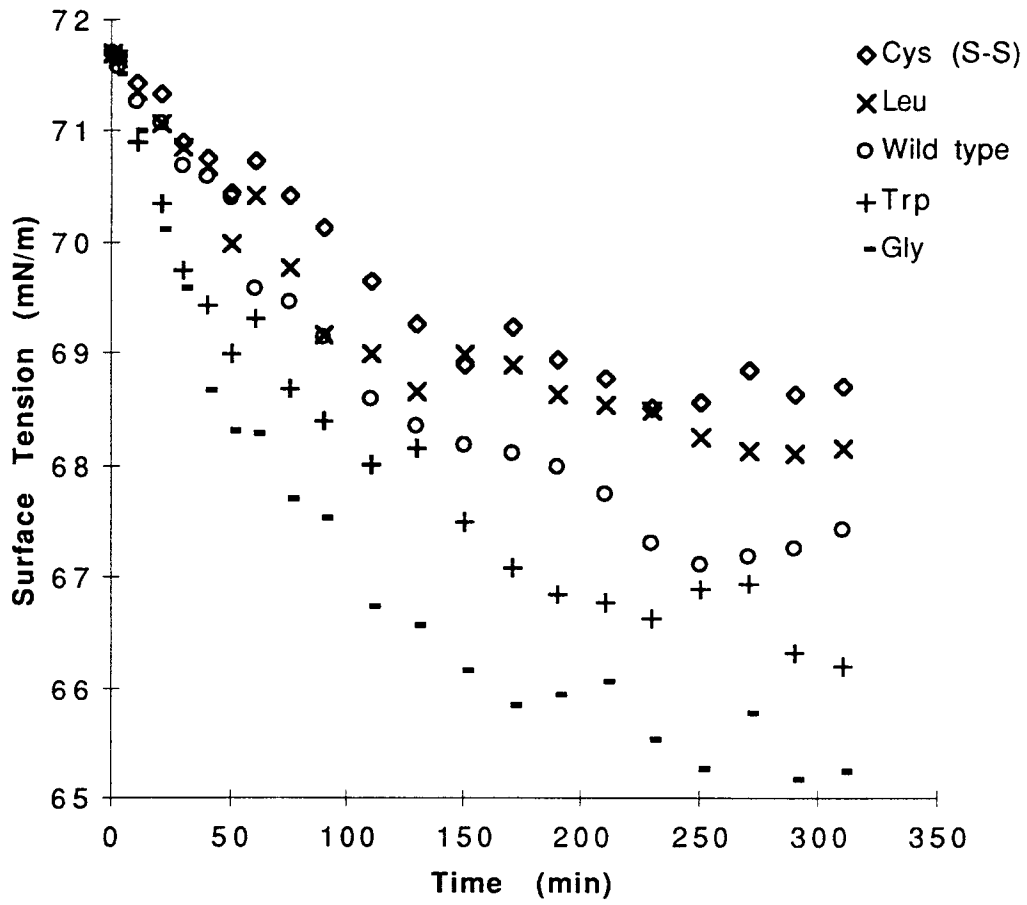


Figure 4.1. Surface tension kinetics of T4 lysozyme and the four stability mutants at a concentration of 0.01 mg/ml.

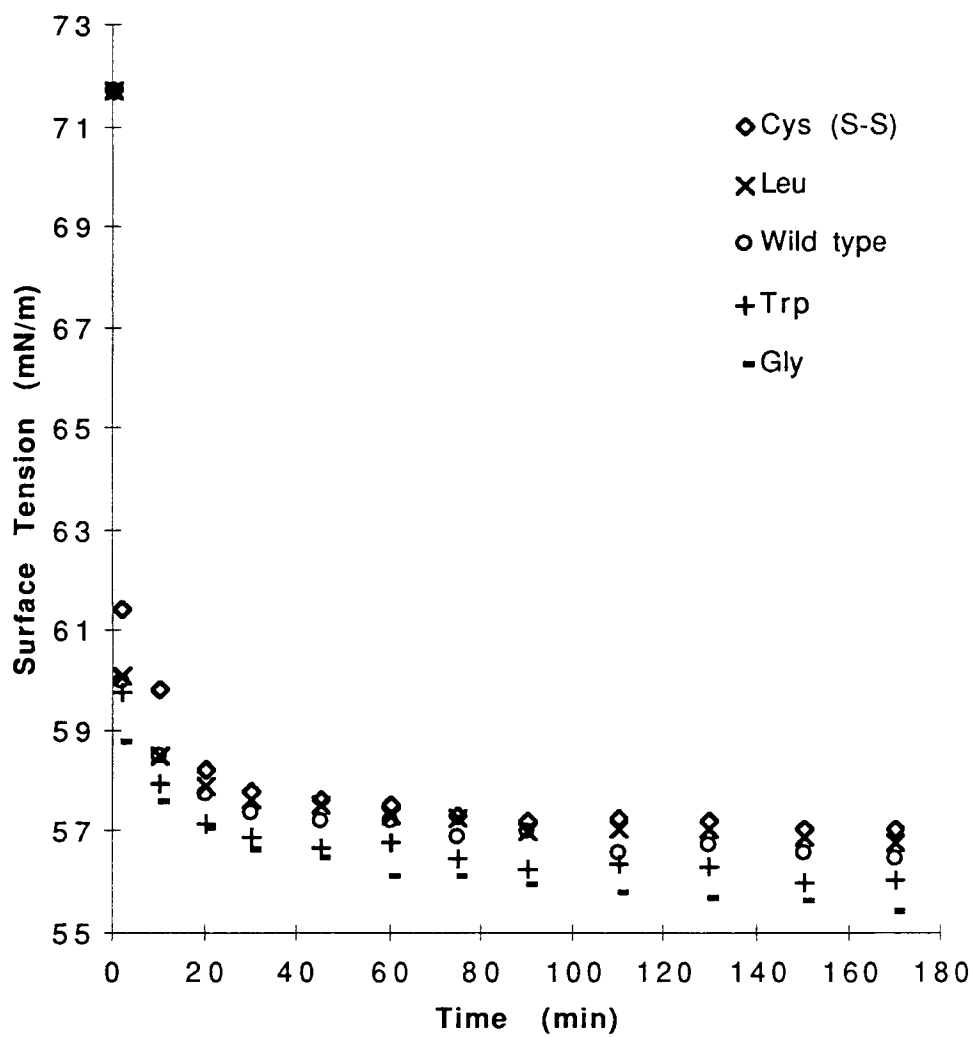


Figure 4.2. Surface tension kinetics of T4 lysozyme and the four stability mutants at a concentration of 1.0 mg/ml.

induction period by suggesting that lysozyme adsorption was not dependent on the protein concentration in the bulk phase right below the surface (subsurface), but rather a mechanism of surface protein unfolding, since the induction periods were longer than the diffusion time. At a concentration of 0.0015 mg/ml Xu and Damodaran (8) found that T4 phage lysozyme adsorbed less than egg-white and human lysozyme, but the induction period was shorter, and the rate and extent of surface pressure increase was greater, than the other two lysozymes. They came to the conclusion that the T4 phage lysozyme more readily undergoes unfolding at the interface, spreads, and occupies a larger surface area. This probably explains why at a concentration of 0.01 mg/ml an induction period was not observed in our experiments.

At low bulk concentrations protein adsorption onto the surface is a relative slow process due to the small amount of molecules in solution. Molecules adsorbed at the interface are more unfolded and spread out so that more surface area is occupied, and further adsorption of molecules from the bulk solution is inhibited. However at high bulk concentrations the abundance of protein molecules results in a quicker adsorption, and the adsorbed molecules have less time to undergo unfolding. This difference is apparent in the data (Figs. 4.1 and 4.2), where at low concentration (0.01 mg/ml) the decrease of surface tension was slower, and the steady-state values were smaller than at high concentration (1.0 mg/ml). These trends for T4 lysozyme are consistent with the results for egg-white lysozyme found in the literature (4, 6, 12).

The surface tension kinetics exhibited by each stability mutant differed somewhat from that of the wild type. In particular the surface tension of the more stable variants was generally higher than that of the less stable mutants for the duration of the experiments. The rate and extent of surface tension changes decreased as $\Delta\Delta G$ increased, with the single exception of those between Ile3 \rightarrow Trp and Ile3 \rightarrow Gly. In wild type lysozyme, Ile 3 contributes to the major hydrophobic core of the C-terminal lobe and helps to link the N- and C-terminal domains (25). The side chain of Trp 3 is the largest

among all the amino acids. It may not be accommodated within the interior of the protein, and thus may be unable to exhibit its full hydrophobic potential for stabilization in the core. This probably gives the mutant more ability to unfold, which may explain why Ile3 → Trp is one of the least stable lysozymes characterized to date (25). Removal of the side chain of Ile 3 tends to create a cavity next to the hydrophobic core (25). This cavity can only be occupied in part by Gly 3, whose side chain is the smallest among all the amino acids. Ile3 → Gly may unfold in a manner exhibiting less steric effects among neighboring molecules than that of Ile3 → Trp. It is possible that for this reason the mutant can pack more closely than Ile3 → Trp at the interface.

Evaluation of the surface tension kinetics exhibited by protein solutions is often accomplished with reference to the following first-order rate equation (11),

$$\ln(\gamma - \gamma_{ss}) / (\gamma_0 - \gamma_{ss}) = -Kt \quad [4.1]$$

where γ_{ss} , γ and γ_0 (mN/m) are the surface tension values at the steady state, at any time t , and at $t = 0$, respectively. K (min^{-1}) is the first-order rate constant.

As observed by Graham and Phillips (11), a plot of Eq. [4.1] usually yields two linear regions with the change of slope occurring at the time that surface protein concentration attains its steady-state value. The initial rapid decrease, which exists while surface concentration is increasing, reflects the penetrating and unfolding of protein molecules in the surface layer. This corresponds to a first-order rate constant of adsorption (K_1). The second slope, which exists when surface concentration is constant, is related to rearrangements of the protein molecules within the surface layer after adsorption has ceased. This is represented by the first-order rate constant of rearrangement (K_2).

Wei *et al.* (6) calculated the first-order rate constant from the surface tension kinetics recorded at 0.01 mg/ml after the induction period, and reported that it correlated with protein stability, suggesting that the decrease in surface tension was due to adsorption of denatured protein. Additionally, they calculated two rate constants from the plots recorded at 1.0 mg/ml, and reported the first kinetic constant to be related to surface hydrophobicity of the protein, and the second to be related to the protein chain length.

Eq. [4.1] can only be applied in the period without diffusion control, to gain information on penetration of proteins into the interface and conformational rearrangement of the adsorbed molecules. According to Penetration Theory (21), at a bulk concentration of 1.0 mg/ml, T4 lysozyme adsorption can be considered as a process without mass transfer limitations. This was based on the calculation of a diffusion-limited adsorption using an apparent diffusion coefficient estimated by Xu and Damodaran (8). The calculation yielded an adsorption rate greater than that seen in any of the adsorption kinetics recorded by McGuire *et al.* at solid surfaces (21).

Considering that steady state was reached after about 90 min for each protein at 1.0 mg/ml, the value of γ_{ss} for each protein was estimated by taking the average of the surface tension values measured after 90 min. A plot of $\ln(\gamma - \gamma_{ss})/(\gamma_0 - \gamma_{ss})$ vs. time up to 90 min was constructed for each protein solution and is shown in Fig. 4.3.

The slopes (rate constants K_1 and K_2) were estimated for each region and are shown in Table 4.1, along with the coefficient of determination for each line.

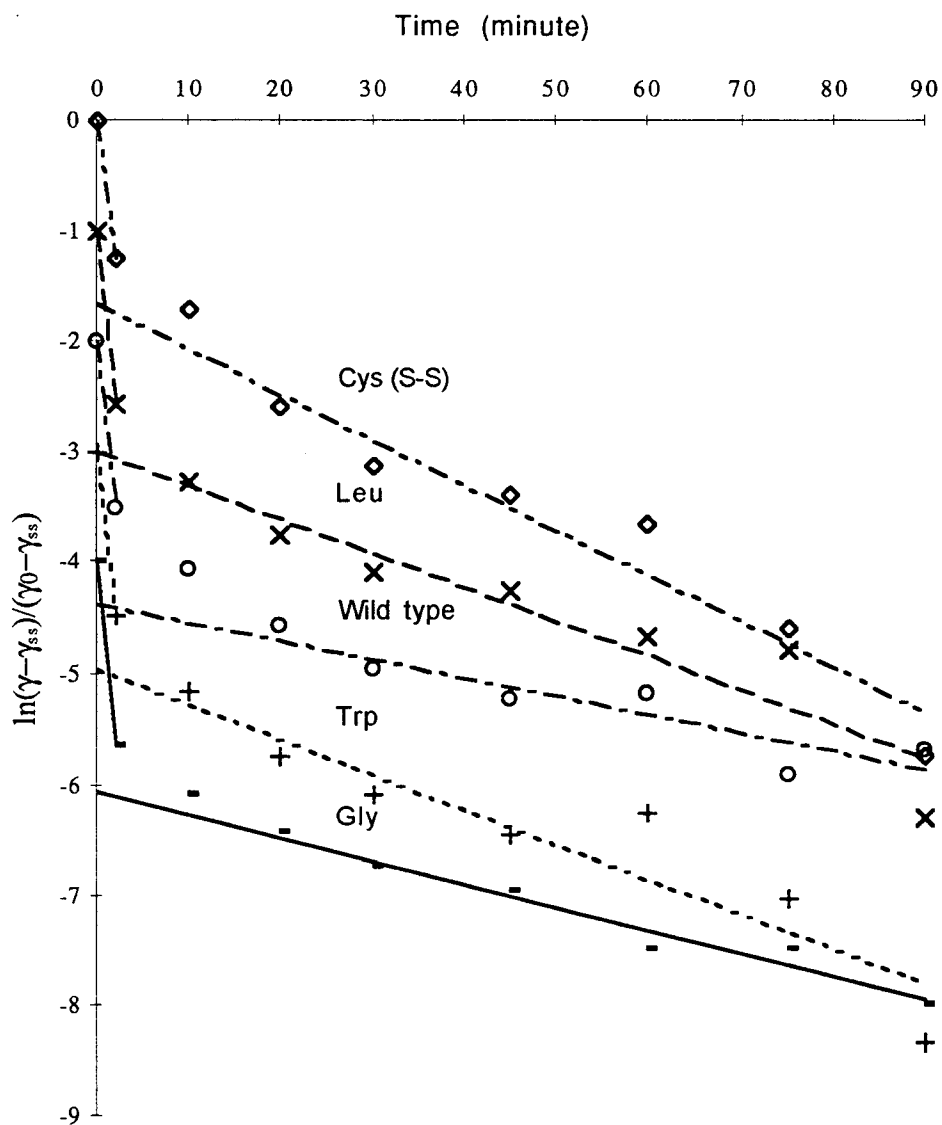


Figure 4.3. Analysis of kinetic plots for each protein at 1.0 mg/ml according to Eq. [4.1]. For the sake of clarity, the curves have been offset from each other by one unit in the vertical axis.

Table 4.1. First-order rate constants K_1 and K_2 for each protein at 1.0 mg/ml.

Proteins	K_1 (min ⁻¹)	R^2 (for K_1)	K_2 (min ⁻¹)	R^2 (for K_2)
Ile3 → Trp	0.733	1.000	0.0316	0.820
Ile3 → Gly	0.819	1.000	0.0212	0.964
Wild type	0.747	1.000	0.0165	0.839
Ile3 → Leu	0.773	1.000	0.0307	0.844
Ile3 → Cys (S-S)	0.614	1.000	0.0411	0.929

At high bulk concentrations (≥ 1.0 mg/ml), the rate constant K_1 had been correlated with an "effective surface hydrophobicity" (6). Higher K_1 values indicate that the proteins are more hydrophobic and therefore adsorb faster to the hydrophobic air-water interface. K_2 corresponds to a first-order rate constant of rearrangement, related to protein molecular weight (6, 28). The five model proteins used in this research differ from each other only in one amino acid at position 3. Considering the total chain length of these lysozymes is 164 amino acids, the surface hydrophobicity and molecular weight should not be significantly affected by one residue. The K_1 and K_2 values in Table 4.1 are similar, given the accuracy of this experimental method.

These model proteins are so similar that evaluation using simple first-order kinetics was not able to provide new information.

The same analysis with the low concentration (0.01 mg/ml) data will be discussed in section 4.3.

4.2 Analysis with Reference to a Simple Kinetic Model

The spreading pressure (Π) of a protein solution is a measure of the difference between its surface tension and that of the protein-free buffer (28),

$$\Pi = \gamma_B - \gamma_P \quad [4.2]$$

where γ_B and γ_P are the surface tension of the pure buffer and the protein solution, respectively.

In order to find a more theoretically sound relationship between spreading pressure and time, we first make use of a simple adsorption kinetic model developed by McGuire *et al.* for T4 lysozyme adsorption to silica surfaces (21). This model evolves from the simple adsorption mechanism illustrated in Fig. 4.4.

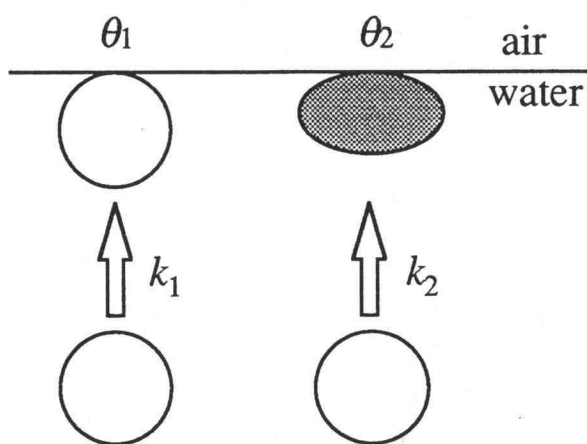


Figure 4.4. A simple mechanism for T4 lysozyme adsorption into one of two states defined by fractional surface coverages θ_1 and θ_2 , where state 2 molecules occupy a greater surface area than molecules adsorbed in state 1. k_1 and k_2 are first-order rate constants for adsorption.

Applied to the present case, protein molecules from a single-component protein solution can adsorb at the air-water interface directly from the solution into one of two states, where state 2 molecules are more tightly bound (via more noncovalent contacts) to the surface than those in state 1. In addition, a state 2 molecule occupies a greater surface area (A_2) than that occupied by a state 1 molecule (A_1). Also shown in Fig. 4.4, k_1 and k_2 are first-order rate constants for adsorption into state 1 and state 2, respectively (21).

4.2.1 Parameter estimation

We will define the maximum adsorbed mass of molecules allowable in a monolayer as Γ_{\max} (mg/m²). θ_1 and θ_2 are respectively, the mass of state 1 and state 2 molecules (mg/m²) adsorbed at any time divided by Γ_{\max} . When the surface is covered, θ_1 and θ_2 must obey the following equations,

$$\theta_1 + a\theta_2 = 1 \quad [4.3]$$

and at any time

$$\Gamma = \Gamma_{\max}(\theta_1 + \theta_2), \quad [4.4]$$

where a is A_2 / A_1 , and Γ (mg/m²) is the actual value of adsorbed mass.

In order to apply this knowledge of $\Gamma = f(\theta_1, \theta_2)$ to understand $\Pi = f(\theta_1, \theta_2)$, we will consider the general case allowing the contributions of state 1 and state 2 molecules to the interfacial energy reduction per area to be different. This is most

appropriate as state 2 molecules are defined as more tightly bound to the surface, which could allow more noncovalent contacts between the molecule and the surface per unit area.

We will define Π_1 and Π_2 as the surface pressures expected when the interface is covered entirely by state 1 and state 2 molecules, respectively, and b as Π_1 / Π_2 . If state 2 molecules are able to make more noncovalent contacts with the surface per unit area, the maximal spreading pressure should correspond to a monolayer of state 2 molecules (i.e., $\Pi_{\max} = \Pi_2 > \Pi_1$). The spreading pressure at any time can then be estimated by

$$\Pi = \Pi_{\max} (b\theta_1 + a\theta_2), \quad [4.5]$$

if Π_{\max} , θ_1 , θ_2 , b and a are known.

Parameters A_1 and A_2 can be approximated as the specific interfacial area that would be occupied by adsorbed "end-on" and "side-on" molecules, respectively, where $A_1 = 1/3.96$ (m²/mg) and $A_2 = 1/2.05$ (m²/mg) based on the dimensions of a lysozyme molecule in solution (21). Therefore $a = 3.96/2.05 = 1.93$.

Graham and Phillips (12) used adsorption isotherms for egg-white lysozyme to show that the steady-state value of surface pressure reached a plateau above a bulk concentration of 0.1 mg/ml. This suggested that at or above 0.1 mg/ml, the protein layer in contact with the air-water interface was saturated; more over, only this layer would affect the surface tension. In the present study we would expect that when the spreading pressure reaches its steady state at a bulk concentration of 1.0 mg/ml, the interface is saturated. Considering the air-water interface as an ideal hydrophobic surface (4), we will assume that these experiments are comparable to those of McGuire *et al.* (21) performed with hydrophobic silica at the liquid-solid interface.

McGuire *et al.* (21) estimated the fraction of state 2 molecules present in a monolayer formed on hydrophobic silanized silica, for the three lysozyme variants, wild type, Ile3 \rightarrow Cys (S-S) and Ile3 \rightarrow Trp. By assuming that the fraction of adsorbed protein in state 2 in the saturated monolayer would be similar in both cases, it becomes possible to estimate θ_1 and θ_2 at the air-water interface for wild type, Ile3 \rightarrow Cys (S-S) and Ile3 \rightarrow Trp by applying the data from McGuire *et al.* (21) along with Eq. [4.3]. In particular, as the fraction of molecules in state 2 approaches $\theta_2 / (\theta_1 + \theta_2)$ at steady state, we have 2 equations and 2 unknown values ($\theta_{1,ss}$ and $\theta_{2,ss}$). Similar to the estimation of steady state values for surface tension (γ_{ss}), the values for spreading pressure at steady state (Π_{ss}) can be calculated from the average of the data after 90 min. The values of Π , $\theta_2 / (\theta_1 + \theta_2)$, θ_1 and θ_2 at steady state are listed in Table 4.2.

Table 4.2. Estimation of θ_1 , θ_2 and Π at steady state for wild type, Ile3 \rightarrow Trp and Ile3 \rightarrow Cys (S-S).

Protein	$\theta_{2,ss} / (\theta_{1,ss} + \theta_{2,ss})$ (from ref. 21)	$\theta_{1,ss}$	$\theta_{2,ss}$	Π_{ss} (mN/m)
Ile3 \rightarrow Trp	0.90	0.0543	0.49	15.493
Wild type	0.37	0.4687	0.2753	15.079
Ile3 \rightarrow Cys (S-S)	0	1	0	14.525

As shown in Table 4.2, a substantial population of adsorbed Ile3 \rightarrow Trp are in state 2, while all Ile3 \rightarrow Cys (S-S) molecules are adsorbed in state 1. For wild type, the amount of state 1 molecules are almost twice as much as those in state 2.

The maximum surface pressure (Π_{\max}) as well as the ratio of surface pressures at steady state (b) can be estimated using Eq. [4.5]. The values for Π , θ_1 , θ_2 and a at steady state are already known. Writing Eq. [4.5] for each protein in any pair taken from Table 3.2, would give two equations with the two unknowns, Π_{\max} and b . Solving the three noncorrelated pairs of equations allowable yielded three estimates of Π_{\max} and b , which are listed in Table 4.3 along with their average values.

Table 4.3. Estimated values of Π_{\max} and b at bulk concentration of 1.0 mg/ml.

Combination of data sets	Π_{\max} (mN/m)	b
Ile3 \rightarrow Trp & Wild type	15.545	0.936
Wild type & Ile3 \rightarrow Cys (S-S)	15.567	0.933
Ile3 \rightarrow Trp & Ile3 \rightarrow Cys (S-S)	15.549	0.934
Average	15.554	0.934

As shown in Table 4.3, estimates of Π_{\max} and b were largely independent of which pair of proteins was used. This is consistent with the assumptions that adsorption at the air-water interface is similar to that at a model hydrophobic solid surface, and that the interface was saturated at steady state. The value of b is smaller than 1, indicating that the interfacial energy reduction per unit area of state 1 molecules is smaller than for state 2 molecules, although this difference is not substantial. However, the steady-state value of surface pressure for Ile3 \rightarrow Gly ($\Pi_{ss} = 16.06$ mN/m) is greater than the value of Π_{\max} estimated with the data of Table 4.2. If we assume that at steady state all Ile3 \rightarrow Gly proteins are adsorbed in state 2 ($k_1 = 0$), then we could estimate $\Pi_{\max, \text{Gly}} = 16.06$ mN/m.

In any event this would agree with the assumption that Ile3 \rightarrow Gly molecules adsorb in a more packed state at the interface than other mutants due to the small side chain of Gly 3.

4.2.2 Model equations and the rate constants

Neglecting the influence of diffusion, equations describing the time-dependent fractional surface coverage of a protein in each of the two states (θ_1 and θ_2) shown in Fig. 4.4 can be written as

$$d\theta_1 / dt = k_1 C (1 - \theta_1 - a\theta_2) \quad [4.6]$$

and

$$d\theta_2 / dt = k_2 C (1 - \theta_1 - a\theta_2), \quad [4.7]$$

where C is the bulk protein concentration (mg/ml). Solving Eqs. [4.6] and [4.7] analytically yields

$$\theta_1 = \frac{1}{1 + ak_2 / k_1} [1 - \exp(-k_1 C - ak_2 C)t] \quad [4.8]$$

and

$$\theta_2 = \frac{k_2 / k_1}{1 + ak_2 / k_1} [1 - \exp(-k_1 C - ak_2 C)t]. \quad [4.9]$$

Therefore an expression for surface pressure as a function of time can be obtained by substituting Eqs. [4.8] and [4.9] into Eq. [4.5], such that

$$\Pi = \Pi_{\max} \frac{b + ak_2/k_1}{1 + ak_2/k_1} [1 - \exp(-k_1C - ak_2C)t] \quad [4.10]$$

The rate constants k_1 and k_2 for each protein were estimated in each case by applying linear regression analysis to the surface pressure kinetics plotted on semi-log coordinates. For this purpose, linear regression analysis was performed on the data for the period 0 to 90 min. The data after 90 min were averaged to obtain the steady state values of surface pressure (Π_{ss}). Eq. [4.10] can be rearranged to

$$\ln(\Pi_{ss} - \Pi) = \ln(\Pi_{ss}) - (k_1C + ak_2C)t, \quad [4.11]$$

where, as $t \rightarrow \infty$, Eq. [4.10] identifies Π_{ss} as

$$\Pi_{ss} = \Pi_{\max} \frac{b + ak_2/k_1}{1 + ak_2/k_1}. \quad [4.12]$$

A plot of $\ln(\Pi_{ss} - \Pi)$ vs. t allows calculation of k_1 and k_2 from the slope and Π_{ss} . The estimated values of k_1 and k_2 , along with $\Delta\Delta G$ at pH = 6.5 and k_2/k_1 for each protein are listed in Table 4.4.

The surface pressure kinetic data, along with their fit to Eq. [4.10], are shown in Fig. 4.5 for each protein. The model (Eq. [4.10]), as shown in Fig. 4.5, does not describe the adsorption very well at short times, probably a result of using a very simple mechanism. It is reasonable to suggest that the rate constants are in fact not constant during the entire adsorption period. In particular, as surface coverage increases, the energy barrier to adsorption may also increase. Such a dependence on surface concentration for

adsorption rate constants has been modeled by Guzman *et al.*, in terms of activation energies for adsorption and desorption (10). Applied to the present case, k_1 and k_2 might be best represented in the form $k_i = k_{i0}\exp(-E_{ai}/RT)$, when E_{ai} , the activation energy for adsorption, is allowed to increase with surface coverage according to $E_{ai} = E_{ai}^0 + \alpha_i \Gamma$. With these data, a satisfactory analysis with Guzman *et al.*'s model is not possible. However, comparison of the adsorption rate constants between wild type T4 lysozyme and its stability mutants can still be made with reference to the simple kinetic model developed here.

Table 4.4. Value of the adsorption rate constants defined in Fig. 4.4, along with the value of $\Delta\Delta G$ for each protein.

Protein	$\Delta\Delta G$ (kcal/mol)	k_2/k_1	$k_1 (\times 10^{-3})$ (ml/mg·min)	$k_2 (\times 10^{-3})$ (ml/mg·min)
Ile3 \rightarrow Trp	-2.8	8.26	3.71	30.7
Ile3 \rightarrow Gly	-2.1	∞	0	27.9
Wild type	0.0	0.60	25.1	15.1
Ile3 \rightarrow Leu	0.4	0.13	50.3	6.44
Ile3 \rightarrow Cys (S-S)	1.2	0	67.3	0

As expected, and shown in Table 4.4, since $k_2/k_1 = \theta_2/\theta_1$ as $t \rightarrow \infty$, the values of k_2/k_1 for Ile3 \rightarrow Cys (S-S), wild type and Ile3 \rightarrow Trp agree quite well with 0, 0.59 and 9.0, respectively, estimated from the values of $\theta_{2,ss}/(\theta_{1,ss} + \theta_{2,ss})$ in Table 4.2. The value of k_2/k_1 for Ile3 \rightarrow Leu lies between that of Ile3 \rightarrow Cys (S-S) and wild type, and this is in agreement with a greater tendency for a protein to adopt state 2 if it is of lower

conformational stability. As all Ile3 \rightarrow Gly protein molecules were constrained as adsorbing in state 2, $k_1 = 0$ and $k_2/k_1 \rightarrow \infty$.

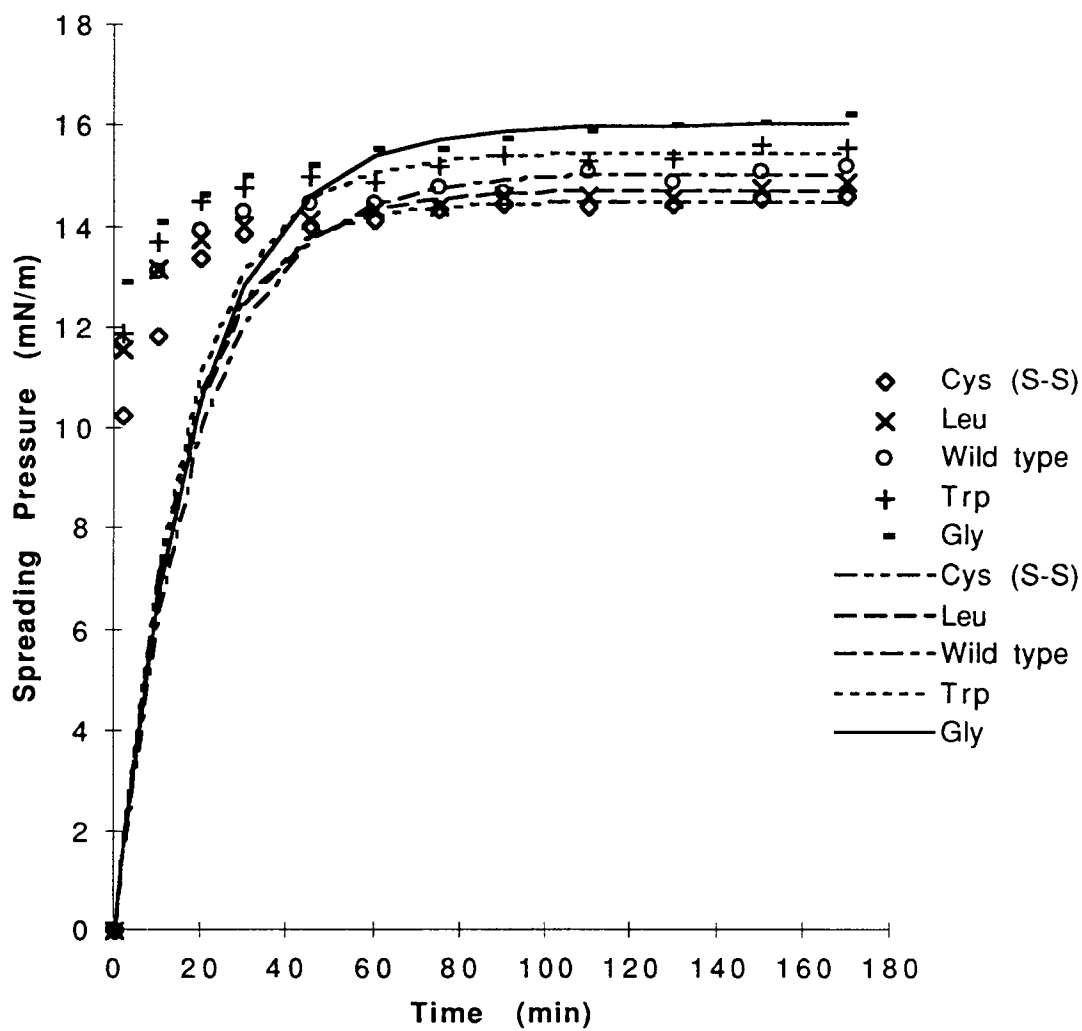


Fig. 4.5. Surface pressure kinetics at a bulk concentration of 1.0 mg/ml. The lines follow Eq. [4.10].

The trend observable in the values of k_1 and k_2 and $\Delta\Delta G$ is clear. We could conclude therefore that a less stable protein would adsorb more tightly, and occupy more interfacial area per molecule, than a more stable protein.

4.3 Mass Transfer Limitations and the Low Concentration Data

The process of adsorption of a protein to a surface generally involves transport of the molecule to the interface, and binding. The transport of protein to a surface is a diffusion process, dependent on bulk concentration and diffusion coefficient (29). In the case of transport-limited adsorption, the rate of protein transport from the solution to the surface is slower than the rate of protein binding to the surface (16). When a fresh interface is created, one could postulate that molecules at the subsurface adsorb to the interface instantaneously, establishing a concentration gradient between the bulk phase and the subsurface. This concentration gradient then provides the driving force for diffusion of molecules from the bulk phase to the subsurface. Solving the equation of continuity for this simple scenario (penetration theory) yields the time dependence of adsorbed mass (16):

$$\Gamma = 2C\sqrt{(Dt/\pi)}, \quad [4.13]$$

where Γ , C , D and t are the adsorbed mass per surface area, bulk concentration, diffusion coefficient and time, respectively.

Xu and Damodaran (8) measured an apparent diffusion coefficient (D_{app}) for T4 lysozyme of $1.5 \times 10^{-12} \text{ m}^2/\text{s}$, which is two orders of magnitude lower than that measured in solution. Using their value of D_{app} as a conservative estimate of the diffusion

coefficient, and assuming, in the most conservative case that all protein molecules adsorb in state 1, the spreading pressure kinetics for diffusion-limited adsorption could be represented by Eq. [4.5] as

$$\Pi = b\Pi_{\max}\theta_1 = 2b\Pi_{\max}C\sqrt{(Dt/\pi)} / \Gamma_{\max}, \quad [4.14]$$

where $\theta_1 = \Gamma/\Gamma_{\max}$ and as before Γ_{\max} is the maximum adsorbed mass in a monolayer ($\Gamma_{\max} = 3.96 \text{ mg/m}^2$).

At high concentration ($C = 1.0 \text{ mg/ml}$), the diffusion-limited adsorption would yield a surface pressure of about 15.2 mN/m after 9 s, which is associated with a rate much greater than that seen in Fig. 4.5. In that case, it would be fair to consider adsorption as occurring without transport limitation. The spreading pressure kinetics measured for each protein at 0.01 mg/ml are plotted in Fig. 4.6, together with the spreading pressure predicted with Eq. [4.14].

It seems that adsorption at a concentration of 0.01 mg/ml may be a transport limited process in the case of the less stable mutants. However, the surface pressure kinetics differed among the protein variants at the beginning of the adsorption process, instead of starting with the same diffusion limited curve. This could be a result of adsorption differences among the protein variants in state 1 and 2, which contribute differently to the interfacial energy reduction; this could also be an indication that the adsorption was not diffusion controlled. The diffusion limited surface pressure kinetics predicted with Eq. [4.14] evolved from an extremely conservative development and are still greater than the spreading pressure kinetic observed in each case, except for that of Ile3 \rightarrow Gly. It may therefore be instructive to consider that the surface pressure kinetics recorded at 0.01 mg/ml were not diffusion-rate controlled.

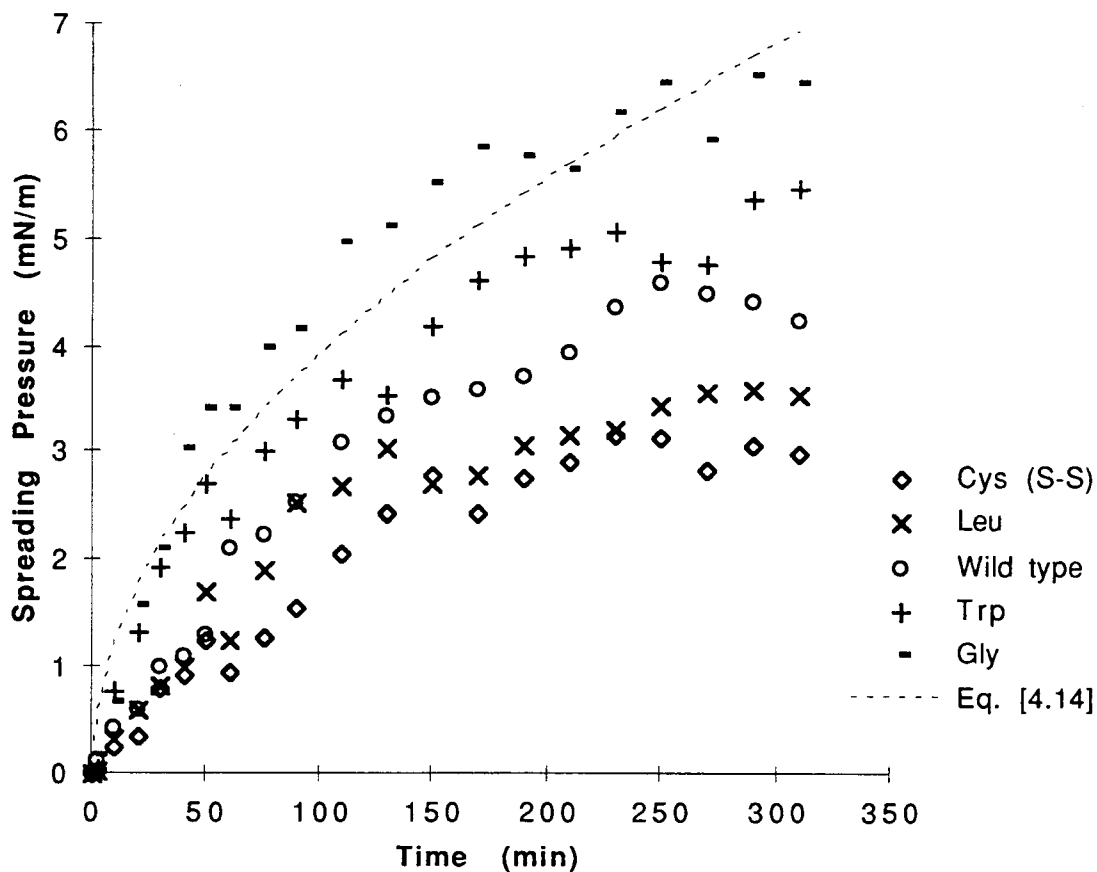


Fig. 4.6. Surface pressure kinetics at a concentration of 0.01 mg/ml, along with the surface pressure predicted with Eq. [4.14].

The surface pressures recorded at low concentration reached steady values that were much smaller than those recorded at high concentration. This agrees with the air-water adsorption isotherm data of egg-white lysozyme from Graham and Phillips (12), in which the surface pressure value at 0.01 mg/ml was about half of the value at 1.0 mg/ml. The same trend was observed by Hunter *et al.* (4) in their surface protein concentration isotherm, leading to the assumption that at low concentrations the surface layer is not

fully covered, not only for different lysozymes, but also for many other proteins (5, 6, 12).

The surface tension kinetics at 0.01 mg/ml shown in Fig 4.1 can also be evaluated with Eq. [4.1]. The value γ_{ss} for each protein was estimated by taking the average of the surface tension values after 2 hours, when the steady state was reached. Fig. 4.7 shows the results of this analysis.

The plots yielded only one linear region, defining one first-order rate constant, K . Wei *et al.* (6) suggested that this rate constant is related to protein stability. The estimated values of K for each protein are shown in Table 4.5, along with the correlation coefficient for each line, and $\Delta\Delta G$.

Table 4.5. Value of the first-order rate constants K , along with the value of $\Delta\Delta G$ for each protein.

Protein	$\Delta\Delta G$ (kcal/mol)	K (min^{-1})	R^2
Ile3 \rightarrow Trp	-2.8	0.0153	0.886
Ile3 \rightarrow Gly	-2.1	0.0135	0.952
Wild type	0.0	0.0120	0.835
Ile3 \rightarrow Leu	0.4	0.0108	0.942
Ile3 \rightarrow Cys (S-S)	1.2	0.0131	0.886

In general, the value of K increases with decreasing $\Delta\Delta G$, except in the case of Ile3 \rightarrow Cys (S-S), which could be associated with the accuracy of the experimental method. However, the trend is not as strong as the kinetic model (Eq. [4.10]) indicated, in regard to the values of k_1 and k_2 at the high concentration (Table 4.4). This could be a result of the

diffusion influence. But most importantly, the relationship between K and protein stability at low concentrations is totally empirical, so we can't expect much.

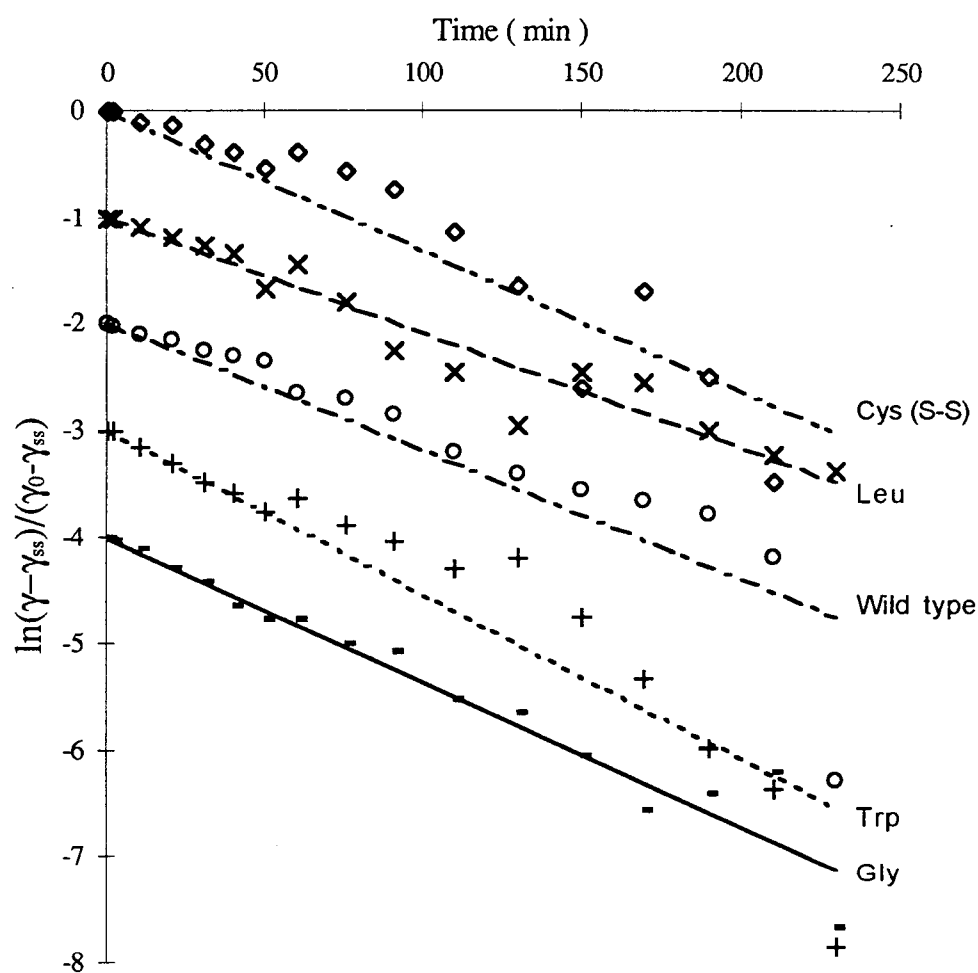


Figure 4.7. Analysis of kinetic plots for each protein at 0.01 mg/ml according to Eq. [4.1]. For the sake of clarity, the curves have been offset from each other by one unit in the vertical axis.

By assuming that the same amount of surface area was covered by each protein variant at steady state, and that the relative amounts of adsorbed protein molecules in state 1 and 2 remained the same as at 1.0 mg/ml, we calculated Π_{\max} and b using Eq. [4.5]. The results are listed in Table 4.6. The data from the period after 240 min were averaged to obtain the steady-state values of surface pressure.

Table 4.6. Estimated values of Π_{\max} and b at 0.01 mg/ml.

Combination of data sets	Π_{\max} (mN/m)	b
Ile3 \rightarrow Trp & Wild type	5.19	0.69
Wild type & Ile3 \rightarrow Cys (S-S)	5.70	0.53
Ile3 \rightarrow Trp & Ile3 \rightarrow Cys (S-S)	5.22	0.58
Average	5.37	0.60

The values of Π_{\max} and b are not as close to each other in this case as at the high concentration (1.0 mg/ml), where the interface was fully covered. This is probably due to the assumptions that the percentage of the surface covered among the protein variants was always the same, and the steady state ratios of adsorbed protein in state 1 and 2 remained the same as at 1.0 mg/ml. The values of b obtained by using this approach were considerably smaller than those from the high concentration ($b = 0.934$). This would suggest that the state 2 protein molecules at low concentrations make more noncovalent bonds with the surface per molecule than those at higher concentrations, resulting in a higher surface pressure if a is kept constant. Alternatively, the value of a at lower protein concentration may actually be larger than 1.93 since the molecules are more spread out. Combining these two factors could explain the lower steady-state values of spreading

pressure and surface adsorbed mass at lower concentrations ($C \leq 0.01$ mg/ml) than at higher concentrations ($C \geq 1.0$ mg/ml): the protein molecules that adsorb may spread out and undergo more structural rearrangement to expose more hydrophobic residues to the air. They may occupy more surface area and build up an energy barrier to limit the arrival of protein molecules from the subsurface, which are already presented at lower amount through the lower concentrations in bulk and eventually the diffusion limitation. Steady state would therefore be reached earlier with less adsorbed mass, and the surface is inefficiently covered with less noncovalent bonds per unit area. It is obvious that the state 1 and 2 molecules are different from those at 1.0 mg/ml resulting in different values of a and b . Therefore in this model mechanism the nature of state 1 and 2 at an interface is dependent upon the bulk concentration.

As with the high concentration, the expression for surface pressure as a function of time (Eq. [4.10]) was also applied to the concentration of 0.01 mg/ml. The semi-log linear regression analysis was performed on the data from 0 min to 240 min. The surface pressure kinetic data at 0.01 mg/ml, along with their fit to Eq. [4.10], are shown in Fig. 4.8 for each protein. With the average values of Π_{\max} and b from Table 4.6 we calculated k_1 and k_2 , and their values are listed in Table 4.7 along with $\Delta\Delta G$ for each protein.

Unlike the case of the high bulk concentration (Fig. 4.5), the model describes the adsorption kinetics relatively well, even at short times. This indicates that the adsorption at 0.01 mg/ml was mainly a kinetically-controlled event. In Table 4.7 the values of k_1 and k_2 are more than one magnitude higher than those in Table 4.4 at 1.0 mg/ml, despite the model's prediction that k_1 and k_2 should remain constant. As proposed earlier, a more accurate model might include the influence of the adsorbed protein molecules on the adsorption rate constants. As shown in Fig 4.5, the model didn't describe the adsorption at short times very well at 1.0 mg/ml, when the surface was barely covered with any proteins. Through the comparison of k_1 and k_2 for both concentrations it becomes obvious that the rate constants at the short times at 1.0 mg/ml were much higher than those

calculated for the whole adsorption period (Table 4.4 and Table 4.7). At low concentration, the surface coverage stayed low through the entire adsorption period, so that the simple model mechanism shown in Fig. 4.4 could describe the whole adsorption process satisfactorily.

Table 4.7. Value of the adsorption rate constants at 0.01 mg/ml, defined in Fig. 4.4, along with the value of $\Delta\Delta G$ for each protein.

Protein	$\Delta\Delta G$ (kcal/mol)	k_2/k_1	$k_1 (\times 10^{-3})$ (ml/mg·min)	$k_2 (\times 10^{-3})$ (ml/mg·min)
Ile3 → Trp	-2.8	3.61	170	610
Ile3 → Gly	-2.1	∞	0	700
Wild type	0.0	0.68	520	350
Ile3 → Leu	0.4	0.09	920	80
Ile3 → Cys (S-S)	1.2	0	1310	0

The same percentage of the surface was not covered for each protein at 0.01 mg/ml, so the values of k_1 and k_2 were not accurately estimated by using the average values of Π_{\max} and b . They still showed the trend with $\Delta\Delta G$ just as they did at 1.0 mg/ml except between Ile3 → Gly and Ile3 → Trp. This might be due to the low k_2/k_1 value calculated for Ile3 → Trp resulting from the use of average Π_{\max} and b values.

As shown in Figure 4.6, the values of spreading pressure were greater for less stable mutants than for more stable ones at any time. Assuming that the relative amount of surface coverage among the protein variants was the same, Figure 4.6 would indicate that more molecules adsorb in state 2 as the variant becomes less stable. Alternatively, if

the surface coverage varied among the proteins, it would be greater for less stable variants than for more stable ones. In each case the less stable variants are revealed more surface active, and we can conclude that the structural stability is a determining factor in protein interfacial behavior.

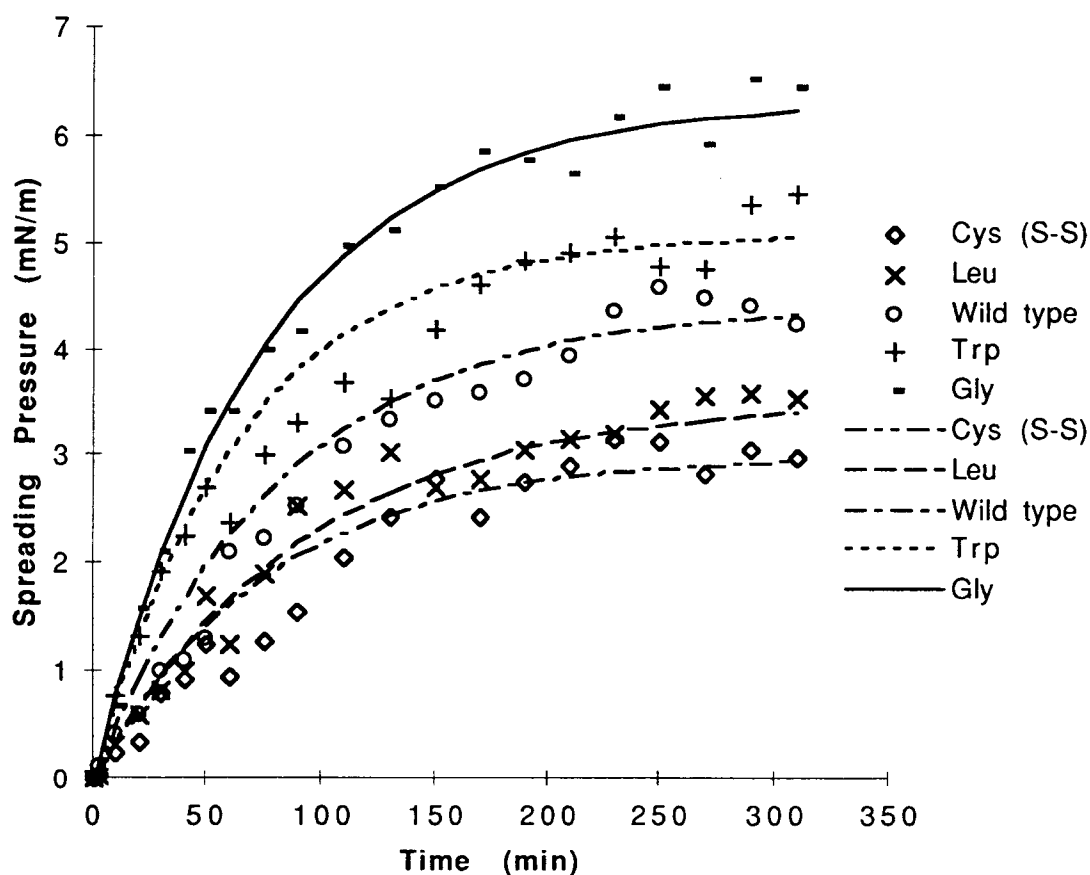


Fig. 4.8. Surface pressure kinetics at a bulk concentration of 0.01 mg/ml. The lines follow Eq. [4.10].

CHAPTER 5

CONCLUSION

Surface tension kinetics at the air-water interface exhibited by selected stability mutants of bacteriophage T4 lysozyme were measured with DuNoüy tensiometry. Analysis of the data using first-order rate equations did not provide an increased understanding of protein adsorption behavior. A comparison of the spreading pressure kinetics to a simple model allowing parallel, irreversible adsorption into two states directly from solution suggested that protein adsorption at an interface is determined largely by the conformational stabilities of proteins. Less stable T4 lysozyme variants tend to adsorb at the air-water interface in a more tightly bound state. Proteins in this state perform more structural rearrangement, and occupy more surface area. This phenomena is more pronounced at lower concentrations.

BIBLIOGRAPHY

1. Norde, Willem. 1986. Adsorption of proteins from solution at the solid-liquid interface. *Adv. Colloid Interface Sci.* **25**:267-340.
2. Kitabatake, Naofumi, and Etsushiro Doi. 1982. Surface tension and foaming of protein solutions. *J. Food Sci.* **47**:1218-1221.
3. Kitabatake, Naofumi, and Etsushiro Doi. 1988. Surface tension and foaming of protein and surfactant solutions. *J. Food Sci.* **53(5)**:1542-1545.
4. Hunter, James R., Peter K. Kilpatrick, and Ruben G. Carbonell. 1990. Lysozyme adsorption at the air/water interface. *J. Colloid Interface Sci.* **137(2)**:462-482.
5. Hunter, James R., Peter K. Kilpatrick, and Ruben G. Carbonell. 1991. β -Casein adsorption at the air/water interface. *J. Colloid Interface Sci.* **142(2)**:429-447.
6. Wei, A. -P., J. N. Herron, and J. D. Andrade. 1990. *The role of protein structure in surface tension kinetics*. D.J.A. Crommelin and H. Schellekens, Eds. From Clone to Clinic. p.305. Amsterdam:Kluwer Academic.
7. Elbaum, Danek, John Harrington, Eugene F. Roth, Jr. and Ronald L. Nagel. 1976. Surface activity of hemoglobin S and other human hemoglobin variants. *Biochim. Biophys. Acta* **427**:57-69.
8. Xu, Shuqian, and Srinivasan Damodaran. 1993. Comparative adsorption of native and denatured egg-white, human, and T4 phage lysozymes at the air-water interface. *J. Colloid Interface Sci.* **159**:124-133.
9. Kato, Akio, and Katsuhide Yutani. 1988. Correlation of surface properties with conformational stabilities of wild-type and six mutant tryptophan synthase α -subunits substituted at the same position. *Protein Eng.* **2(2)**:153-156.
10. Guzman, Roberto Z., Ruben G. Carbonell, and Peter K. Kilpatrick. 1986. The adsorption of proteins to gas-liquid interfaces. *J. Colloid Interface Sci.* **114(2)**:536-547.
11. Graham, D.E., and M. C. Phillips. 1979. Proteins at liquid interfaces: I. kinetics of adsorption and surface denaturation. *J. Colloid Interface Sci.* **70(3)**:403-414.

12. Graham, D.E., and M. C. Phillips. 1979. Proteins at liquid interfaces: II. adsorption isotherms. *J. Colloid Interface Sci.* **70(3)**:415-426.
13. Narsimhan, Ganesan, and Farooq Uraizee. 1992. Kinetics of adsorption of globular proteins at an air-water interface. *Biotechnol. Prog.* **8(3)**:187-196.
14. Douillard, Roger, and Jacques Lefebvre. 1990. Adsorption of proteins at the gas-liquid interface: models for concentration and pressure isotherms. *J. Colloid Interface Sci.* **139(2)**:488-499.
15. Lundström, Ingemar. 1985. Models of protein adsorption on solid surfaces. *Progr. Colloid Polymer Sci.* **70**:76-82.
16. Krisdhasima, Viwat, Joseph McGuire, and Robert Sproull. 1992. Surface hydrophobic influences on β -lactoglobulin adsorption kinetics. *J. Colloid Interface Sci.* **154(2)**:337-350.
17. Krisdhasima, Viwat, Pravina Vinaraphong, and Joseph McGuire. 1993. Adsorption kinetics and elutability of α -lactalbumin, β -casein, β -lactoglobulin, and bovine serum albumin at hydrophobic and hydrophilic interfaces. *J. Colloid Interface Sci.* **161**:325-334.
18. Kondo, Akihiko, and Ko Higashitani. 1992. Adsorption of model proteins with wide variation in molecular properties on colloidal particles. *J. Colloid Interface Sci.* **150(2)**:344-351.
19. Kato, Akio, and Shuryo Nakai. 1983. Hydrophobicity determined by a fluorescence probe method and its correlation with surface properties of proteins. *Biochem. Biophys Acta* **624**:13-20.
20. Nakai, Shuryo. 1983. Structure-Function relationship of food proteins with an emphasis on the importance of protein hydrophobicity. *J. Agric. Food Chem.* **31(4)**:676-683.
21. McGuire, Joseph, Marie C. Wahlgren, and Thomas Arnebrant. 1995. Structural stability effects on the adsorption and dodecyltrimethylammonium bromide-mediated elutability of bacteriophage T4 lysozyme at silica surfaces. *J. Colloid Interface Sci.* **170**:182-192.
22. Grütter, M. G., and Brian W. Matthews. 1982. Amino acid substitutions far from the active site of bacteriophage T4 lysozyme reduce catalytic activity and suggest

- that the C-terminal lobe of the enzyme participates in substrate binding. *J. Mol. Biol.* **154**:525-535.
23. Matthews, Brian W., and S. J. Remington. 1974. The three dimensional structure of the lysozyme from bacteriophage T4. *Proceedings of National Academy of Science USA* **71(10)**:4178-4182.
 24. Alber, Tom, and Brian W. Matthews. 1987. Structure and thermal stability of phage T4 lysozyme. *Methods Enzymol.* **154**:511-533.
 25. Matsumura, Masazumi, Wayne J. Beckel, and Brian W. Matthews. 1988. Hydrophobic stabilization in T4 lysozyme determined directly by multiple substitutions of Ile 3. *Nature* **334**:406-410.
 26. CSC Scientific Co., Inc.. 1988. "Operating Instructions: CSC-duNoüy Tensiometer CSC Nos. 70535 and 70545". p. 1. CSC Scientific Fairfax, VA.
 27. Weser, C.. 1980. Measurement of interfacial tension and surface tension - general review for practical man. *GIT Fachzeitschrift für das Laboratorium* **24**:642-648&734-742.
 28. Suttiprasit, Prasert, Viwat Krisdhasima, and Joseph McGuire. 1992. The surface activity of α -lactalbumin, β -lactoglobulin, and bovine serum albumin. *J. Colloid Interface Sci.* **154(2)**:316-326.
 29. Andrade, J. D., V. Hlady, and A. P. Wei. 1992. Adsorption of complex proteins at interfaces. *Pure & Appl. Chem.* **64(11)**:1777-1781.
 30. Podhipleux, Nilobon, Viwat Krisdhasima, and Joseph McGuire. 1995. Molecular charge effects on protein behavior at hydrophobic and hydrophilic solid surfaces. *Food Hydrocoll.* **in press**.